Wave Breaking Events and their link to Rossby Wave Packets and Atmospheric Blockings during Southern Hemisphere Summer

Iago Pérez-Fernández[1], Marcelo Barreiro[1], Noémie Ehstand[2],Emilio Hernández-García[2], Cristobal López[2].

[1]*Departamento de Ciencias de la atmósfera y Física de los Océanos, Facultad de Ciencias, Universidad de la República, Montevideo, Uruguay.*

[2]*Instituto de Fisica Interdisciplinar y Sistemas Complejos (IFISC), CSIC-UIB. Palma de Mallorca, Spain.*

Corresponding author: Iago Pérez-Fernández (iperez@fisica.edu.uy)

Key Points:

- Large-scale wave breaking events caused by propagating Rossby Wave Packets do not usually last enough to develop into an atmospheric block.
- Years with La Niña and positive Southern Annular Mode favor large-scale wave breaking activity linked to short-lived Rossby Wave packets.
- Near 17% of blocking events appear preceded by a wave breaking event but most of them are not linked to propagating Rossby Wave Packets.

Abstract

Rossby Wave packets (RWPs) are atmospheric perturbations located at upper levels in mid-latitudes which, in certain cases, terminate in Rossby Wave Breaking (RWB) events. When sufficiently persistent and spatially extended, these RWB events are synoptically identical to atmospheric blockings, which are linked to heatwaves and droughts. Thus, studying RWB events after RWPs propagation and their link with blocking is key to enhance extreme weather events detection 10-30 days in advance. Hence, here we assess (i) the occurrence of RWB events after the propagation of RWPs, (ii) whether long-lived RWPs (RWPs with a lifespan above 8 days, or LLRWPs) are linked to large-scale RWB events that could form a blocking event, and (iii) the proportion of blocking situations that occur near RWB events. To do so, we applied a tracking algorithm to detect RWPs in the Southern Hemisphere during summertime between 1979-2020, developed a wave breaking algorithm to identify RWB events, and searched for blocking events with different intensities. Results show that LLRWPs and the other RWPs displayed large-scale RWB events around 40% of the time, and most RWB events in both distributions last around 1-2 days, which is not long enough to identify them as blocking situations. Nearly 17% of blockings have a RWB event nearby, but barely 5% of blockings are linked to RWPs, suggesting that propagating RWPs are not strongly linked to blocking development. Lastly, large-scale RWB events associated with RWPs that lasted less than 8 days are influenced by the Southern Annular Mode and El Niño-Southern Oscillation.

Plain Language Summary

When an atmospheric wave breaks in the upper level of the atmosphere, it modifies the wind flow and local weather conditions. If these wave breaking events are sufficiently big and stable, they can produce atmospheric blocking events, which are linked to heatwaves and drought development. In this study, we assess if a link between wave breaking events caused by long-lived traveling atmospheric waves (atmospheric waves that last more than 8 days in the atmosphere) and blocking events development exists during Southern hemisphere summer. Independently of the duration of the wave packets, near 4 out of 10 times they cause very extensive wave breaking events, but they do not last long enough to be considered an atmospheric blocking. Oppositely, nearly 20% of blocking events manifest nearby a wave breaking event independently of the strength of the block, but these wave breaking events do not seem to be linked to traveling wave packets. Therefore, this study suggests that traveling atmospheric waves are not directly related to the development of atmospheric blockings. Also, the occurrence of extensive wave breaking events caused by traveling atmospheric waves that last less than 8 days are affected by phenomena like El Niño or the Southern Annular Mode.

Keywords — Rossby Wave Packets, Wave Breaking, ENSO, SAM, Atmospheric Blocking

1 Introduction

Rossby Wave Packets (RWPs) are synoptic scale perturbations that appear in the upper atmosphere of mid-latitudes. During their propagation, these packets travel by downstream development mechanisms, transporting large quantities of energy in the process (Tu-Cheng Yeh 1949, Chang and Yu 1999; Chang 2000). RWPs play an important role in the global atmospheric circulation because they are related to storm track variability (Souders *et al.*, 2014a). In addition, they are precursors of extreme weather events such as heatwaves, extreme rainfall (Chang 2005; Grazzini and Vitart 2015, O'brien and Reeder 2017, Wirth *et al.*, 2018) and extratropical cyclone development (Chang *et al.*, 2005, Sagarra and Barreiro 2020). Also, during their propagation they increase the uncertainty of middle-long range forecast (from 3 to >10 days in advance) in the areas they cross (Zheng *et al.*, 2013). Normally, these packets tend to last between 3-6 days in the atmosphere but, under certain circumstances, they can last up to 2-3 weeks before disappearing (e.g. Pérez *et al.*, 2021). When RWPs have a lifespan longer than 8 days, they are referred to as long-lived RWPs or LLRWPs (Grazzini and Vitart 2015).

The lifespan and propagation of the RWPs greatly depend on the potential vorticity gradients and the locations of diabatic heating sources (Grazzini and Vitart 2015). Potential vorticity gradients shape the waveguide where the RWPs propagate, such that a very zonal and intense jet with

narrow potential vorticity gradients favor the development of very stable RWPs (Chang & Yu 1999, Souders *et al.,* 2014b, Wirth *et al.,* 2020), whereas weaker gradients damp or stop the wave packets propagation (Grazzini and Vitart 2015).

Due to the lack of large baroclinically unfavorable areas in the Southern Hemisphere, RWPs are easier to detect than in the Northern Hemisphere (Grazzini and Vitart 2015). In addition, during austral summer (December to March) the jet stream displays a very zonal and narrow wind flow, which acts as a waveguide where RWPs propagate (Hoskins & Ambrizzi, 1993; Chang, 1999), and facilitates RWPs detection. Pérez *et al.,* (2021) showed that the Southern Annular Mode (SAM) heavily influences the development of LLRWPs during austral summer, such that years with positive SAM disfavor LLRWPs development whereas negative SAM favor them. Conversely, El Niño-Southern Oscillation (ENSO) influence was found to be less robust.

When RWPs reach the end of their life cycle they can “break”, causing an irreversible mixing of potential vorticity fields over a longitudinally confined region (Simmons and Hoskins 1978, McIntyre and Palmer 1983, 1984). As a result, high potential vorticity air intrudes the troposphere and/or low potential vorticity air enters in the stratosphere, causing the development of potential vorticity anomalies that can either remove or reverse the usual potential vorticity meridional gradients. This process is called Rossby Wave Breaking or RWB (McIntyre and Palmer 1983, 1984, Berrisford *et al.*, 2007, Masato *et al.,* 2011). RWB events are key to the air mass exchange between the troposphere and the stratosphere (Holton et al., 1995), and are considered as potential precursors of weather regime transitions (Michel and Riviére 2011) that can increase the prediction skill of precipitation (Ryo et al., 2013). In addition, RWB events share some characteristics with atmospheric blocking. In fact, RWB events that show a spatial and temporal scale similar to atmospheric blocking are synoptically recognized as a blocking (Berrisford et a*l., 20*07). An atmospheric blocking event is a nearly-stationary large-scale pattern in the pressure field arising from the reversal of the westerly wind flow, and it is stable enough to last from several days to weeks in the atmosphere (Rex, 1950, Patterson *et al.*, 2019). Its appearance is linked to the development of extreme weather events such as heatwaves or droughts (Woollings, *et al., 2*018). Nonetheless, even if we find some RWB events prior to the onset of some atmospheric blockings (Altenhoff *et al.,* 2008), not all events are associated with blocking (Hitchman and Huesmann 2007, Masato *et al., 20*13).

There are two main types of RWB (Thorncroft *et al.*, 1993), one is cyclonic RWB, where low potential temperature or “cold” air from the dynamical tropopause moves eastward and equatorward to the west of high potential temperature air or “warm” air, whereas “warm” air goes poleward and westward. The other is anticyclonic RWB, where the equatorward and westward movement of low potential temperature air is to the east of the poleward and eastward movement of the “warm” air. Each morphology of wave breaking implies different changes in synoptic circulation. Anticyclonic RWB occurs with much more frequency than cyclonic RWB

because RWPs propagating in the tropopause tend to break in an anticyclonic fashion (Thorncroft *et al.,* 1993; Peters and Waugh 1996, 2003).

Several studies of RWB were done for the Northern Hemisphere (e.g. Strong and Magnusdottir 2008, Masato *et al*., 2011, Michel and Riviére 2011, Ryoo *et al.,* 2013). For example, Thorncroft *et al.* (1993) found that RWB frequency is influenced by processes that alter the wind flow. In that regard, Strong and Magnusdottir (2008) concluded that the positive phase of the Northern Annular Mode is associated with anticyclonic RWB, whereas its negative phase is linked to cyclonic RWB. In the Southern Hemisphere, Berrisford *et al., (*2007) showed that RWB in mid latitudes wintertime is concentrated in the east Pacific, whereas during summertime RWB episodes are less frequent and are confined to the west Pacific. This is in (qualitative) agreement with the observed location of Southern hemisphere blocking. Gong *et al.*, (2010) studied the influence of SAM and ENSO on RWB breaking during austral spring-summer, and found that the positive phase of SAM shows higher wave breaking activity than the negative. Additionally, Wang and Magnusdottir (2010) observed that anticyclonic and cyclonic RWB frequency is affected by the changes in background flow caused by ENSO events.

A question still unanswered is the relationship between the occurrence of RWB and the propagation of RWPs in the Southern hemisphere, as well as whether RWPs can cause RWB events that can trigger atmospheric blocking development. Thus, the aim of this research is to study the detection and evolution of RWB events after the propagation of transient RWPs, with special emphasis on large-scale RWB. In addition, we classified the RWB considering whether their associated RWPs is a LLRWPs or not. This is done in order to assess whether the wave breaking events caused by LLRWPs share different characteristics as the those found for the rest of the RWPs, and study whether RWB events that occur after the dissipation of a LLRWPs are linked to the development of atmospheric blocking.

The paper is organized as follows. Section 2 describes the datasets and the methodologies for tracking RWPs, detecting RWB events, as well as blockings. Section 3 focuses on the link between RWB and RWPs, section 4 on the interannual variability of RWB events and the potential impact of global climate modes, and section 5 assesses the link between atmospheric blocking and RWB events. Finally, section 6 presents a summary of the study.

2 Data and methodology

2.1 Data

In this study, we used ERA 5 Reanalysis (Hans *et al.,* 2020), with an horizontal resolution of 0.25º x 0.25º and daily frequency. The region of study consists of the mid-latitudes of the Southern Hemisphere, during austral summer (December to March or December-March) between 1979-2021 as done in previous studies (Sagarra and Barreiro 2020, Pérez *et al.,* 2021). Thus, we have 41 seasons available for the analysis.

RWPs propagate in the upper atmosphere of mid-latitudes and manifest as meanders of the jet stream. During their propagation, they produce a series of troughs and ridges that travel confined to a certain latitudinal band, moving mainly eastward during austral summer (Chang 1999). Thus, by computing the envelope of the meridional wind speed at 300 hPa (V_{300env}), we can characterize these transient RWPs. To calculate the V_{300env}, we followed the methodology specified in Pérez *et al.*, (2021). Next, due to the fact that RWPs propagation is mostly zonal during December-March season (Chang 1999), we averaged the V_{300env} data between the latitudinal range of 40-65ºS.

Regarding the detection of RWB events, as in previous studies, we have used the potential vorticity field in isentropic coordinates, searching for areas where the usual meridional potential vorticity gradient either disappears or is inverted. The computation of the potential vorticity field was performed following Hoskins *et al.*, (1985), using daily temperature and wind speed at 300 hPa interpolated to the isentropic coordinates of 330ºK.

Also, to characterize the interannual variability and amplitude of the global climate modes, we used the Oceanic Niño Index for ENSO, and the Antarctic Oscillation index for SAM. Both datasets are publicly available in the NOOA website (https://origin.cpc.ncep.noaa.gov/).

2.2 Description of Rossby Wave Packet tracking algorithm

The RWPs are detected using a tracking algorithm, based on the maximum envelope technique (Grazzini and Vitart 2015, Sagarra and Barreiro 2020, Pérez *et al.*, 2021). This algorithm searches for areas with the highest daily values of $V_{300env,}$ identifying the center of activity of the RWPs, and then follow the propagation of the wave packets to the east, assuming that they travel between 15-45ºE per day. Before applying the tracking algorithm, we filter out small values of V_{300env} to avoid tracking noise. Although there is no optimum threshold because there are no physical properties that separate one wave packet from another (Souders *et al.*, 2014b), here we applied a minimum threshold of 19 m/s. Pérez *et al.*, (2021) show that the tracking of RWPs is not sensitive to the choice of threshold between 17-21 m/s.

It is also worth pointing out that the tracking algorithm only follows transient RWPs that is, RWPs that propagate eastwards and have a zonal wavenumber between 4-11, which corresponds to the transient structures of the Southern Hemishere (Trenberth 1981). Therefore, the algorithm cannot track stationary RWPs, or those RWPs with a wavenumber ≤3. Hereafter, when we talk about RWPs, we are referring to these transient RWPs.

After the algorithm finishes tracking all the RWPs of the season, it uses proximity criteria to link trajectories of the RWPs that were interrupted, and then measures the characteristics of the tracked wave packet: longitudinal extension, areas of formation/dissipation, lifespan and propagation speed. The full description of the algorithm is available in Pérez *et al.*, (2021).

Finally, for the subsequent analysis, the tracked RWPs are classified in LLRWPs (lifetime >8 days) and short lived RWPs or SLRWPs (lifetime<=8 days).

2.3 Rossby Wave Breaking detection algorithm and validation

As we mentioned in section 2.1, RWB events manifest in the upper atmosphere in areas where the usual meridional gradient of potential vorticity either disappears or reverses. We can detect these areas by locating where the potential vorticity contour lines overturn following isentropic coordinates (McIntyre and Palmer 1983). Previous studies in the Southern Hemisphere followed potential vorticity contours in the isolines between 310-350ºK (Ndarana and Waugh 2010 a, b, Strong and Magnusdottir 2008) because they represent the dynamical tropopause between the high latitudes and the subtropics (Ndarana and Waugh 2010 a).

We choose to study RWB events that occur in the potential vorticity of -2 PVU (1 PVU = 10^{-6} $m^2\ s^{-1}\ K\ kg^{-1}$) on the 330ºK isosurface. The reason to chose this specific isosurface is because it is a transitional region between the isosurface 310-350ºK, where anticyclonic and cyclonic shear have been found (Ndarana and Waugh 2010 a, b).

In order to identify RWB events we developed an objective algorithm based on the methodology of Barnes and Hartmann (2012). The steps of the algorithm are the following:

1.- Representation of the -2 PVU contour line for day t, and retention of the longest contour line. This is done to avoid the detection of isolated potential vorticity “bubbles” as part of RWB events.

2.- Identification of areas where -2 PVU contours crosses more than 2 times the same longitudinal section. These points are referred as wave breaking points.

3.- If there are wave breaking points closer than 500 km from each other we assumed that these points belong to the same wave breaking event (Barnes and Hartmann 2012).

4.- Retention of RWB events that have a longitudinal extension>= 5º. This avoids registering meridionally extended potential vorticity tongues that do not show overturning.

5.- Classification of the RWB event regarding their orientation. This is done by measuring the latitudinal mean of the 4 most eastward and westward overturning points of the RWB episode. In the Southern Hemisphere, cyclonic RWB events have their western-most overturning point located equatorward, while their east-most overturning point is poleward. By contrast, in anticyclonic RWB events their eastern-most overturning point are equatorward whereas their west-most overturning point are poleward. Thus, if the latitudinal mean of their most westward points of the contour is closer to poleward latitudes than the observed at the most eastward points, we assume that the wave packet shows an anticyclonic shear, whereas if the most westward points are closer to the equator than the most eastward points, the breaking event is

classified as cyclonic RWB. An example of the application of the RWB tracking algorithm can be seen in figure 1.

6.- Measurement of the RWB characteristics: longitudinal and latitudinal extension of the event, day of detection, and type of RWB shear.

7.- Repeat steps 1-6 for the following days until all the data is analyzed.

Given the few studies reported on RWB for the Southern hemisphere it is important first to ensure that the detection algorithm works as expected. To do so, we first tracked wave breaking events in the December-March season only between 1979-2008, and compared our results against previous studies (Ndarana and Waugh 2010 a,b, Wang and Magnusdottir 2010).

2.4 Linking large-scale Rossby wave breaking events to Rossby Wave Packets

In this section we explain the methodology used to link RWB activity to the dissipation of RWPs. At the moment of writing this article, the authors were not able to find a study which links RWB events with RWPs in the Southern Hemisphere.

Before describing the methodology, it is important to highlight that in this section we will only consider large-scale RWB, that is RWB events with a longitudinal extension of 1000 km (~15º in mid latitudes) or above (Barnes and Hartmann 2012). This is done in order to retain wave breaking events that can strongly affect the large-scale atmospheric circulation and have a spatial scale similar to atmosphere blocking, (11º of extension, Patterson *et al*., 2019).

The methodology used for linking RWPs with RWB events has the following steps:

1.-Apply the RWB tracking algorithm at day T_f, being T_f the day when a RWP finished its propagation.

2.-If the algorithm detects the beginning of a RWB event located between $X_f \pm 2000$ km, being X_f the longitudinal section where the algorithm located a RWPs before stopping its propagation, we assume that the wave breaking event registered is linked to the RWP that stopped its propagation and we proceed to step 3. If the described condition is not fulfilled, we continue looking for RWB events for the following days. If by day T_{f+4} we do not find a RWB event that matches the described condition, we assumed that the RWP did not show a RWB episode and finish the search. Oppositely, if after applying the wave breaking detection algorithm we detect two or more RWB event which are in the range $X_f \pm 2000$ km, we select the RWB whose geographical center is closer to the area of dissipation of the RWP.

3.-We register the day when a RWB event is detected as $T_{n,}$ and applied the RWB tracking algorithm at day $T_{n.+1}$. If a RWB event exists with geographical center within 20º (~1400 km**)** of distance or less from the wave breaking episode found at day $T_{n,}$, we assume that this event is an

extension of the RWB event found the previous day. Else, we infer that the RWB episode only lasted for a day.

4.- Step 3 is repeated for the following days until we stop finding wave breaking events that fulfill the condition specified in step 2.

5.- We save the same characteristics of the RWB events detailed in section 2.3 as well as the day a RWB event was detected after the dissipation of a RWP, and how many days lasts the RWB associated to a RWP.

In step 2, we search for RWB events in the area located between $X_f \pm 2000$ km because even if X_f signals the center of the RWP, the packet has a certain longitudinal extension, and thus the RWB event does not have to necessarily appear near X_f. Barnes and Hartmann (2012) considered that RWB events that are within 2000 km of the geographical center of the RWB belong to the same episode, hence, in this study we look for RWB events that are up to 2000 km of distance from the area of dissipation of the RWPs. On the other hand, we chose to search for events a few days after the end of the RWPs propagation because it is possible that before disappearing the RWPs might be stationary for a few days. By examining the evolution and behavior of several potential vorticity fields several days after the dissipation of a RWPs we chose an upper limit of 4 days.

Additionally, in step 3 we used a distance of 1400 km to search for the continuation of a RWB episode, because using a longer distance can cause the algorithm to select a wrong wave breaking event that is too far away from the original episode that is being tracked.

Figure 2 shows an example of the methodology followed to link RWPs with RWB events.

2.5 Linking atmospheric blocking to large-scale Rossby wave breaking events

Lastly, we compared the proportion of large-scale RWB events that are present nearby the development of an atmospheric blocking event. In order to detect the occurrence of atmospheric blocking events, we use the methodology of Tibaldi and Moldenti (1989), but modified to consider a range of latitudes in the Southern Hemisphere following Mendes *et al*., (2011). This technique measures two geopotential height meridional gradients from a central latitude, one to the north (GHGN) and another one to the south (GHGS) by using expressions 1 and 2.

$$(1)\ GHGN = (Z(\lambda,\theta_1) - Z(\lambda,\theta_N)) / (|\theta_1 - \theta_N|)$$

$$(2)\ GHGS = (Z(\lambda,\theta_S) - Z(\lambda,\theta_2)) / (|\theta_S - \theta_2|)$$

Where

$\theta_N = 40^oS + \Delta$

$\theta_2 = 50^oS + \Delta$

$\theta_1 = 55^oS + \Delta$

$\theta_S = 65^oS + \Delta$

$Z(\lambda,\theta)$ is the geopotential height at 500 hPa in a latitude θ and longitude λ, and Δ belongs to the set {-10,-7.5, -5, -2.5, 0, 2.5, 5, 7.5, 10}. If on a specific day, at a given longitude λ, GHGN > 0 and GHGS < -10 m/degree of latitude for, at least, one value of Δ, the longitude is considered to be "blocked". Note that, we measure GHGN and GHGS using slightly different expressions from Mendes *et al*., (2011). The definition chosen here implies a stronger requirement on the blocked longitudes than the one considered in the latter study.

Once instantaneous, local, blocked conditions have been identified, additional persistence and spatial extension requirements must be imposed to define atmospheric blocking events. Various thresholds have been used in the literature. Patterson *et al.*, (2019) define an atmospheric blocking event when they detect a blocked longitudinal sector covering, at least, 11º and when this condition persists for a minimum of 4 days in the atmosphere. Mendes *et al*., (2011), use a minimum spatial extent of 7.5º in longitude and persistence of 5 days. In our study, we registered events that have a minimum longitudinal extension of 7.5, 10, 12.5 and 15º and display a minimum lifespan of 4-5 days, measuring the longitude of detection, lifetime and zonal extension of the blocks. This is done in order to assess whether the proportion of atmospheric blocks that might be linked to RWB is sensitive to the blocking conditions. Hence, events that last at least 4 days with a longitudinal extension of 7.5º are most frequent and represent blocking-like situations, that is, the persistent reversal of the westerly wind flow that are not sufficiently extensive to be considered as a blocking event, whereas those that last more than 5 days and have a zonal extension of at least 15º are considered the strongest blocks of the dataset.

In section 5, we first verify that our algorithm works as intended by measuring the frequency of occurrence and areas of formation of blocking events in our period of study, comparing the results to those obtained in Mendes *et al.*, (2011). We then study the potential links between large-scale RWB events and blocking events by identifying the events which occur on the same day and such that their respective geographical center are separated by a maximum of 2000 km. The fulfillment of the latter conditions ensures that the RWB event is present near the development of the atmospheric block. Lastly, we determine how many of the RWB events that occur near an atmospheric block are associated to propagating RWPs. This analysis assesses the proportion of atmospheric blocks that are associated to large-scale RWB activity, and whether RWB activity linked to propagating RWPs is directly linked to the development of atmospheric blocking events.

3 Rossby wave breaking events and their relationship to Rossby Wave Packets

3.1 Verification of Rossby Wave Breaking algorithm

The analysis of RWB events during the December-March season between 1979-2008 detected a total of 659 RWB events in December, 470 in January, 413 in February and 581 events in March. As for the orientation of the RWB events, 22% of the total wave breaking activity belongs to cyclonic RWB, and the rest to anticyclonic RWB.

Figure 3 shows the longitudinal distribution of RWB frequency of occurrence. The maximum RWB activity occurs in the western Pacific (between 140-200º E), and the lowest activity is located near 0ºE. These results indicate that RWB is weakest at the jet entrance in the Atlantic basin, and largest at the jet exit, consistent with the fact that RWPs activity occurs in the Atlantic-Indian basin where the strong jet acts as waveguide (Pérez *et al.*, 2021).

Additionally, figure 4 shows that the main area of anticyclonic RWB detection is located in the western Pacific, as reported by Ndarana and Waugh (2010b). Nonetheless, we also observe two secondary areas of maximum anticyclonic RWB activity, one located in the Indian Ocean and the second in the eastern Pacific-western Atlantic. The latter is in agreement with Ndarana and Waugh (2010b), but these authors found very little anticyclonic RWB activity in the Indian Ocean during December-February. Nonetheless, Ndarana and Waugh (2010b) found significant RWB activity in that region during March-May, suggesting that the differences with our results are explained because of our consideration of March in the summer season. Thus, overall our results are close to those observed in Ndarana and Waugh (2010b), providing a verification of our RWB algorithm. It is worth pointing out that in our case the areas of RWB frequency have wider meridional extension than those found in Ndarana and Waugh (2010b), because our algorithm registers the whole latitudinal area where the overturning potential vorticity is detected.

3.2 Characteristics of Rossby Wave Breaking after Rossby Wave Packet propagation

For the Southern Hemisphere summertime during 1979-2021, a total of 1256 RWPs were found, which corresponds to around 30 per season. Moreover, 141 were LLRWPs, that is about 11% of the total RWPs. From the 141 LLRWPs, 45% have associated large-scale RWB, whereas for the SLRWPs (1115 cases) this proportion is close to 39%. In both cases RWB events show anticyclonic shear: 79% (76%) of the RWB episodes detected after the propagation of a LLRWP (SLRWP) show anticyclonic RWB.

Figure 5 displays the frequency of occurrence of RWB events as a function of longitude that happened after the end of a LLRWPs/SLRWPs. When we focus on the RWB events linked to the end of LLRWPs propagation, (figure 5a), we observe that the distribution of these events is displaced eastward. As Pérez *et al*., (2021) showed, LLRWPs tend to last longer and propagate further into the western Pacific due to an extension of the jet wave guide modulated by the SAM.

On the other hand, most of the wave breaking events that appear after the dissipation of SLRWPs, (figure 5b), tend to occur between 120-180ºE, which corresponds to the Indian-western Pacific sector. This is similar to the results obtained in previous studies (Ndarana and Waugh 2010 a,b). The results found here are consistent with these results, such that an extended jet stream allows LLRWPs to propagate further east and break in the Pacific ocean, instead of in the eastern Indian ocean sector. Thus, RWB events associated with LLRWPs tend to occur in the middle-eastern Pacific basin, which could imply that long-lived packets might be precursors of weather regime transitions affecting conditions in South America.

Figure 6 shows temporal and spatial characteristics of the RWB events detected after the dissipation of LLRWPs and SLRWPs. In figure 6a we display the number of days that pass until a RWB event is detected after the dissipation of a RWP. The two distributions are similar, that is, most of the RWB events occur the same or the next day after the RWP dissipation, although we observe more dispersion in the LLRWPs distribution. Additionally, figure 6b shows the lifespan of the RWB events, indicating that most of the RWB events last between 1-2 days, and that there are no significant differences between both distributions. Nonetheless, when we compare the zonal extension of the wave breaking events, (figure 6c), RWB events that occur after the propagation of SLRWPs cover larger longitudinal extensions compared to those observed after LLRWPs. RWB events linked to LLRWPs show a median longitudinal extension of 22º, and a interquartile range of 12º, whereas RWB associated to SLRWPs have a median of 26.5º and display an interquartile range of 15º. A Kruskall-Wallis test applied to the datasets of figure 6c, indicates that the distributions are significantly different, at 5% level of significance.

Hence, these results suggest that RWB events caused by SLRWPs cover larger longitudinal extensions of the atmosphere compared to those produced by LLRWPs. Nonetheless, neither LLRWPs or SLRWPs seem to be directly related to atmospheric blocking development because, even if the associated RWB events have similar spatial scales to a blocking event, they tend to last only about 1-2 days, too short to lead to blocking (see also section 5).

4 Interannual variability of Rossby Wave Breaking events associated to LLRWPs/SLRWPs

The interannual variability in the occurrence of RWB associated to LLRWPs and SLRWPs is shown in figure 7. Both time series show large year-to-year variability. In the case of LLRWPs, the number of annual RWB events range from 0 to 11, while for SLRWPs it ranges from 6 to 32. During certain periods the frequency of occurrence of RWB associated to the LLRWPs and SLRWPs seem to be out of phase, but no significant correlation has been found between the two time series.

Figure 8 shows the temporal evolution of the RWB events linked to LLRWPs together with the SAM/ENSO indices, this is, the Antarctic Oscillation Index for SAM and the Oceanic Niño Index for ENSO. A correlation analysis indicates that there is no linear relationship between the number of RWB events linked to the dissipation of LLRWPs with SAM or ENSO. It is also

worth noting that one reason that can influence the results is that we have several years without RWB activity linked to LLRWPs, which can increase the difficulty of finding significant correlation between the timeseries of RWB events linked to LLRWPs and SAM or ENSO activity.

On the other hand, the interannual variability of RWB events linked to SLRWPs is correlated with SAM/ENSO indices (Figure 9). Years with positive SAM have a higher frequency of occurrence of RWB linked to SLRWPs, and the opposite occurs in years with negative SAM. This is reflected in a Pearson correlation coefficient value of 0.25 between the Antarctic Oscillation Index and the RWB events linked to SLRWPs, which is statistically significant at 10% level (using Student t-test). Moreover, a similar analysis indicates that the correlation between the Oceanic Niño Index and RWB events linked to SLRWPs is -0.35, statistically significant at 5% level. Thus, La Niña years tend to favor the development of RWB events, whereas El Niño years do the opposite. In agreement, Wang and Magnusdottir (2010) and Gong et *al.*, (2010) concluded that RWB in the tropical/subtropical Pacific is increased during La Niña events, and this was associated to a strong local decrease in the zonal wind. At the same time Barreiro (2017) found that El Niño events tend to favor the RWPs propagation. Therefore, El Niño seems to induce large scale background conditions that favor the propagation of RWPs and, by extension, diminishes the occurrence of RWB, whereas the wind flow decrease during La Niña disfavors the propagation of RWPs and propitiate the occurrence of RWB events.

5 Link between atmospheric blocking and large-scale Rossby Wave Breaking

Results of section 3.2 suggest that the link between RWB associated with RWPs and blocking is not obvious because these RWB events tend to last 1 or 2 days. Here we look further into the relationship between RWB and blockings.

Table 1 shows the number of blocking events found as a function of the persistence and longitudinal extension considered. For the less restrictive criteria (blocks that last at least 4 days and with a minimum longitudinal extension of 7.5º) there are 263 events between 1979-2020 summertime, which corresponds to around 6 blocking events per season. This large number of events reflects the fact that these criteria cause the finding of more blocking-like situations than atmospheric blocks. On the other hand, for the most intense blocks (lifespan of 5 or more days and with a minimum extension of 15º) there are 55 events, this is, a mean of 1.3 events per year. As expected, we observe a decrease in blocking events as the conditions become more restrictive.

It is worth mentioning that we find a mean of 3 atmospheric block events per year when we follow the criteria of Mendes *et al.*, (2011), which is similar to the number they found (between 2.9-3.1 events per year).

In addition, when we focus on the detection areas of blockings, we find that near 50% of the events appear at the central-western Pacific basin (181-240ºE) independently of the zonal extension and persistence of the event. On the other hand, there is a secondary area of blocking development in the eastern Indian basin (121-180ºE), where we find around 23-38% of the blocking events, showing the highest (lowest) values during the strongest (weakest) blocking events. Oppositely, we barely detect any blocking in the western south-Atlantic (300-359ºE) or the central Indian basin (0-60ºE). These results are summarized in table 2 and are in accordance with the observations in Hendes *et al*., (2011).

The search for large-scale RWB associated to the formation of an atmospheric block reveals that the latter appear close to a RWB event between 15-18% of the times independently of the strength and stability of the block (not shown). Also, in agreement with the results of section 3.2, we only found RWB linked to propagating RWPs near the development of an atmospheric block around 3-6% of the times, and it does not seem to depend on the intensity and stability of the block.

To summarize, RWB events are present in the atmosphere around 1 out of 5 times an atmospheric block is detected in the atmosphere, but these RWB events do not seem to be related with the propagating RWPs. Thus, propagating RWPs do not seem to be directly linked to the development of atmospheric blocks. We recall that here we described propagating RWPs as those with speed between 15-45º/day eastward, a zonal number between 4-12 days, and lifespan larger than three days.

6 Summary and conclusions

Rossby Wave Breaking events are atmospheric perturbations that interfere in the wind and energy flow, and under certain circumstances they can cause an atmospheric block, leading to the development of heatwaves or droughts. In this work, an algorithm to track overturning regions of potential vorticity was developed in order to identify Rossby Wave breaking areas that are linked to the dissipation of transient Rossby Wave Packets.

We found that both long-lived Rossby Wave Packets and short-lived Rossby Wave packets tend to show wave breaking events around 40% of the time, although this number is slightly higher for long-lived packets. Rossby Wave breaking events that occur preceded by long-lived Rossby Wave Packets tend to manifest at the center-eastern part of the Pacific basin, and are less zonally extended compared to the wave breaking events associated with the rest of the packets. Therefore, changes in weather regime conditions caused by wave breaking events that are linked to long-lived Rossby Wave Packets are more likely to occur at the south of South America. Moreover, wave breaking events linked to Rossby Wave Packets tend to last between 1-2 days in the atmosphere for both long-lived and short-medium lived packets. Thus, wave breaking events produced by propagating RWPs do not seem to be directly linked to the development of atmospheric blocks.

Previous studies have found that negative SAM years are characterized by a larger number of long-lived Rossby Wave Packets due to the extension of the Atlantic-Indian basin jet wave guide into the Pacific (Pérez *et al.,* 2021). Here we report that the frequency of wave breaking linked to long-lived Rossby Wave packets do not seem to be affected by SAM nor ENSO. On the contrary, positive SAM conditions and La Niña events favor the development of wave breaking episodes after the propagation of short-lived RWPs. Pérez e*t al.,* (2021) concluded that the frequency of occurrence of long-lived Rossby Wave packets is negatively correlated with the number of short-lived Rossby Wave Packets. Thus, years with positive SAM conditions cause a decrease in the number of long-lived Rossby Wave Packets and an increase of short-lived packets. Consequently, the amount of Rossby Wave breaking events linked to Rossby Wave Packets is expected to increase in years with positive SAM events. In addition, results also suggest that RWB events are more common during years with La Niña.

Finally, we assess whether Rossby Wave Breaking events appear near the development of atmospheric blocks, and found that around 1 out of 5 times a blocking event develops, a Rossby Wave Breaking event is present. However, Rossby Wave Breaking linked to propagating Rossby Wave Packets do not seem to be associated to atmosphere blocking development. Therefore, blocking event development during southern hemisphere summertime might be linked to other atmospheric perturbations not considered in this study such as stationary Rossby Wave packets, propagating wave packets with very low wavenumber (1-3), or they might be triggered by other atmospheric processes.

Data availability Statement

ERA5 reanalysis data are freely available in the Copernicus Climate Data Store https://cds.climate.copernicus.eu/, whereas ENSO and SAM indexes are available at https://origin.cpc.ncep.noaa.gov/. The wind envelope amplitude of the RWPs used in this study is publicly available at https://doi.org/10.5281/zenodo.5714192, and a script describing how to obtain wind envelope data from meridional wind speed at https://doi.org/10.5281/zenodo.5724656.

Acknowledgments

This project has received funding from the European Union's Horizon 2020 research and innovation programme under the Marie Skłodowska-Curie grant agreement No 813844 (ITN CAFÉ). NE, CL and EHG acknowledge grant PID2021-123352OB-C32 funded by MCIN/AEI/ 10.13039/501100011033 FEDER/UE.

References

Altenhoff, M, A., Martius, O., Croci-Maspoli, M.,Schwierz, C & Davies,C,H. (2008) Linkage of atmospheric blocking and synoptic-scale Rossby waves: a climatological analysis, Tellus A: Dynamic Meteorology and Oceanography, 60(5), 1053-1063, https://doi.org/10.1111/j.1600-0870.2008.00354.x

Barnes, A, E and Hartmann, L,D. (2012) Detection of Rossby wave breaking and its response to shifts of the midlatitude jet with climate change. *Journal of Geophysical Research,* 117(D9). https://doi.org/10.1029/2012JD017469

Berrisford, P., Hoskins, J, B and Tyrlis, E. (2007) Blocking and Rossby Wave Breaking on the Dynamical Tropopause in the Southern Hemisphere. *Journal of the Atmospheric Sciences*,64(8), 2881-2898. https://doi.org/10.1175/JAS3984.1

Chang, E. K. M. (1999) Characteristics of wave packets in the upper troposphere. Part II: Seasonal and hemispheric variations. *Journal of Atmospheric Sciences*, *56*(11), 1729-1747. https://doi.org/10.1175/1520-0469(1999)056<1729:COWPIT>2.0.CO;2

Chang, E. K. M., & D. B. Yu. (1999) Characteristics of wave packets in the upper troposphere. Part I:Northern Hemisphere winter. *Journal of Atmospheric Sciences*, *56*(11), 1708-1728. https://doi.org/10.1175/1520-0469(1999)056<1708:COWPIT>2.0.CO;2

Chang, E. K. M. (2000) Wave Packets and Life Cycles of Troughs in the Upper Troposphere: Examples from the Southern Hemisphere, Summer Season of 1984/1985. *Monthly Weather Reviewer*, *128*(1), 25-50. https://doi.org/10.1175/1520-0493(2000)128<0025:WPALCO>2.0.CO;2

Chang, E. K. M. (2005) The Impact of Wave Packets Propagating across Asia on Pacific Cyclone Development. *Monthly Weather Review*, *Vol* 133(7) 1998-2015. https://doi.org/10.1175/MWR2953.1

Gong, T., Feldestein, B. S., Luo, D. (2010) The Impact of ENSO on Wave Breaking and Southern Annular Mode Events.*Journal of the atmospheric Sciences*, 67(9), 2854-2870. https://doi.org/10.1175/2010JAS3311.1

Grazzini, F and Vitart F. (2015) Atmospheric predictability and Rossby wave packets. *International Journal. of the Royal . Meteorological. Society*, 141(692), 2793-2802. https://doi.org/10.1002/qj.2564

Hans, H., Bell, B., Berrisford, P., Hirahara, S., Horány, A.,Muñoz-Sabater, *et al.* (2020) The ERA5 global reanalysis. *Royal Meteorological Society*, 146(730), 1999-2049. https://doi.org/10.1002/qj.3803

Hitchman, H. M., and Huesmann,S,A. (2007) A seasonal clima-tology of Rossby wave breaking in the 320–2000-K layer. J.Atmos. Sci., 64(6), 1922–1940. https://doi.org/10.1175/JAS3927.1

Holton, J. R., Haynes , H P., McIntyre, E. M., Douglass,R, A., Roodm. B., R and Pfister, L. (1995) Stratosphere–troposphere exchange. Rev. Geophys., 33(4), 403–439. https://doi.org/10.1029/95RG02097

Hoskins,J,N., Ambrizzi, T. (1993) Rossby Wave Propoagation on a Realistic Longitudinally Varying Flow. Journal of the Atmospheric Sciences, 50(12). https://doi.org/10.1175/1520-0469(1993)050<1661:RWPOAR>2.0.CO;2

513 Hoskins J,B., McIntyre E,M., Robertson W,A. (1985) On the use and significance of isentropic potential vorticity maps. Q. J. R.
514 Meteorol. Soc. 111(470), 877–946. https://doi.org/10.1002/qj.49711147002

515 Masato, G., Hoskins, J,B., Woollings,T. (2011) Wave breaking characteristics of mid-latitude blocking. *Quarterly Journal of the*
516 *Royal Meteorological Society*, 138(666), 1285-1296. https://doi.org/10.1002/qj.990

517 Masato,G, Hoskins,J,B., Woollings,T. (2013) Wave-Breaking Characteristics of Northern Hemisphere Winter Blocking: A Two-
518 Dimensional Approach. *Journal of Climate*, 26(13), 4535-4549. https://doi.org/10.1175/JCLI-D-12-00240.1

519 Mendes, M. C. D., Cavalcanti, I. F., & Herdies, D. L. (2011) Southern Hemisphere atmospheric blocking diagnostic by ECMWF
520 and NCEP/NCAR data. *Revista Brasileira de Meteorologia*, 27(3), 263-271. https://doi.org/10.1590/S0102-77862012000300001

521 Michel, C and Riviére, G (2011) The Link between Rossby Wave Breaking and Weather Regime Transitions. *Journal of The*
522 *Atmospheric Sciences*, 68(8), 1730-1748. https://doi.org/10.1175/2011JAS3635.1

523 McIntyre, E, M., and Palmer,T,N (1983) Breaking planetary waves in the stratosphere. Nature, 305, 593–600.
524 https://doi.org/10.1038/305593a0

525 McIntyre, E, M and Palmer, T.N., Palmer, (1984) The “surf zone” in the stratosphere. J. Atmos. Terr. Phys., 46(9), 825–839.
526 https://doi.org/10.1016/0021-9169(84)90063-1

527 Ndarana, T and Waugh, D., (2010a) The link between cut-off lows and Rossby wave breaking in the Southern Hemisphere. Q.J.R
528 Meteorol. Soc, 136(649), 869-885. https://doi.org/10.1002/qj.627

529 Ndarana, T and Waugh, W,D (2010b) A climatology of Rossby Wave Breaking on the Southern Hemisphere Tropopause.
530 Journal of the Atmospheric Sciences,Vol 68, 798-811. https://doi.org/10.1175/2010JAS3460.1

531 O’Brien L., & Reeder, J, M. (2017) Southern Hemisphere Summertime Rossby Waves and Weatherin the Australian Region.
532 *Quarterly Journal of the Royal Meteorologica Society*. *143*(707), 2374-2388. https://doi.org/10.1002/qj.3090

533 Patterson, M., Bracegirdle, T., & Woollings, T. (2019) Southern Hemisphere atmospheric blocking CMIP5 and future changes in
534 the Australia-New Zealand sector. *Geophysical Research Letters*,46(15), 9281–9290. https://doi.org/10.1029/2019GL083264

535 Peters, D., and Waugh, W, D. (1996) Influence of barotropic shear on the poleward advection of upper-tropospheric air. *J. Atmos.*
536 *Sc*, 53(21), 3013–3031. https://doi.org/10.1175/1520-0469(1996)053<3013:IOBSOT>2.0.CO;2

537 Peters, D., and Waugh, W, D. (2003) Rossby wave breaking in the Southern Hemisphere wintertime upper troposphere. *Mon.*
538 *Wea. Rev*., 131(11), 2623–2634. https://doi.org/10.1175/1520-0493(2003)131<2623:RWBITS>2.0.CO;2

539 Pérez, I., Barreiro, M., & Masoller,C. (2021) ENSO and SAM influence on the generation of long episodes of Rossby Wave
540 Packets during Southern Hemisphere summer. *Journal of Geophysical Research: Atmospheres*, 126(24).e2021JD035467
541 https://doi.org/10.1029/2021JD035467

542 Rex, D. F. (1950) Blocking action in the middle troposphere and its effect upon regional climate. Tellus, 2(3), 196–211.
543 https://doi.org/10.3402/tellusa.v2i4.8603

Ryoo, J-M., Kaspi, Y., Waugh, W , D., Kiladis, N, G., Waliser, E, D., Fetzer, J, E and Jinwon, K. (2013) Impact of Rossby Wave Breaking on U.S. West Coast Winter Precipitation during ENSO Events,*Journal of Climate*,26(17), 6360-6382. https://doi.org/10.1175/JCLI-D-12-00297.1

Sagarra, R., & Barreiro, M. (2020) Characterization of extratropical waves during summer of the Southern Hemisphere. *Meteorologica*, 45(2), 63-79. https://hdl.handle.net/20.500.12008/33550

Simmons, J. A., and Hoskins,J,B (1978) The life cycles of somenonlinear baroclinic waves. J. Atmos. Sci., 35(3), 414–432. https://doi.org/10.1175/1520-0469(1978)035<0414:TLCOSN>2.0.CO;2

Souders, B. M., Colle, A. B., & Chang, M. K. E. (2014a) The climatology and characteristics of Rossby Wave Packets using a feature-based tracking technique. Monthly Weather Review, 142(10), 3528–3548. https://doi.org/10.1175/MWR-D-13-00371.1

Souders, B. M., Colle, A. B., & Chang, M. K. E. (2014b) A Description and Evaluation of an Automated Approach for Feature-Based Tracking of Rossby Wave Packets. Monthly Weather Review, 142(10), 3505–3527. https://doi.org/10.1175/MWR-D-13-00317.1

Strong, C and Magnusdottir, G. (2008) Trophospheric Rossby Wave Breaking and the NAO/NAM, *Journal of the Atmospheric Sciences*,65(9), 2861-2876 https://doi.org/10.1175/2008JAS2632.1

Tibaldi, S. and Molteni, F (1990) On the operational predictability of blocking. Tellus A, 42, 343-365. https://doi.org/10.1034/j.1600-0870.1990.t01-2-00003.x

Thorncroft, D. C., Hoskins, J, B, and McIntyre,E,M (1993) Two paradigms of baroclinic-wave life-cycle behaviour. Quart. J. Roy. Meteor. Soc., 119(509), 17–55.https://doi.org/10.1002/qj.49711950903

Trenberth, E. K. (1981). Observed Southern Hemisphere Eddy Statistics at 500 mb: Frequency and Spatial Dependence. J*ournal of Atmospheric Science*, 38(12), 2585–2605. https://doi.org/10.1175/1520-0469(1981)038<2585:OSHESA>2.0.CO;2

Wang, Y and Magnusdottir, G (2010) Tropospheric Rossby Wave Breaking and the SAM, 24(8), 2134-2146, https://doi.org/10.1175/2010JCLI4009.1

Wiedenmann, M,J., Lupo,R,A., Mokhov, I, I and Tikhonova, A, E. (2002) Journal of Climate, 15(23), 3459-3473. https://doi.org/10.1175/1520-0442(2002)015<3459:TCOBAF>2.0.CO;2

Wirth, V., Riemer, M., Chang, E, K, M., & Martius, O. (2018) Rossby Wave Packets on the Midlatitude waveguide- a review. *Monthly Weather Review*, *146*(7), 1965-2001. https://doi.org/10.1175/MWR-D-16-0483.1

Wirth, V. (2020) Waveguidability of idealized midlatitude jets and the limitations of ray tracing theory. Weather Climate Dynamics, 1, 111–125. https://doi.org/10.5194/wcd-1-111-202

Woollings, T., Barriopedro, D., Methven, J., Son, S.-W., Martius, O., Harvey, B., et al. (2018) Blocking and its response to climate change. Current Climate Change Reports, 4, 287–300. https://doi.org/10.1007/s40641-018-0108-z

Yeh, T. C. (1949) On energy dispersion in the atmosphere. Journal of Meteorology, 6(1), 1–16. https://doi.org/10.1175/1520-0469(1949)006<0001:OEDITA>2.0.CO;

Zheng, M., Chang, E. K., & Colle, B. A. (2013) Ensemble sensitivity tools for assessing extratropical cyclone intensity and track predictability. *Weather and forecasting*, *28*(5), 1133-1156.. https://doi.org/10.1175/WAF-D-12-00132.1

Tables

	7.5º L	10ºL	12.5ºL	15ºL
4d	263	212	168	123

	7.5ºL	10ºL	12.5ºL	15ºL
5d	142	107	79	55

Table 1. Number of blocking events found using different criteria, (d) refers to minimum lifespan in days and (L) the minimum longitudinal extension in degrees of the atmospheric blocks detected.

	Eastern South-Atlantic-western Indian basin (0-60ºE)	Central Indian basin (61-120ºE)	Eastern Indian basin (121-180ºE)	Western Pacific basin (181-240ºE)	Eastern Pacific basin (241-300ºE)	Western South-Atlantic (301-359ºE)
4d 7.5º L	10	16	63	118	38	18
5d 15º L	1	2	20	27	4	1

Table 2. Number of summertime blocking events between 1979 and 2020 in the area of study for two blocking detection criteria: (d) refers to minimum lifespan of the event in days, and (L) to its minimum longitudinal extension in degrees.

Figures

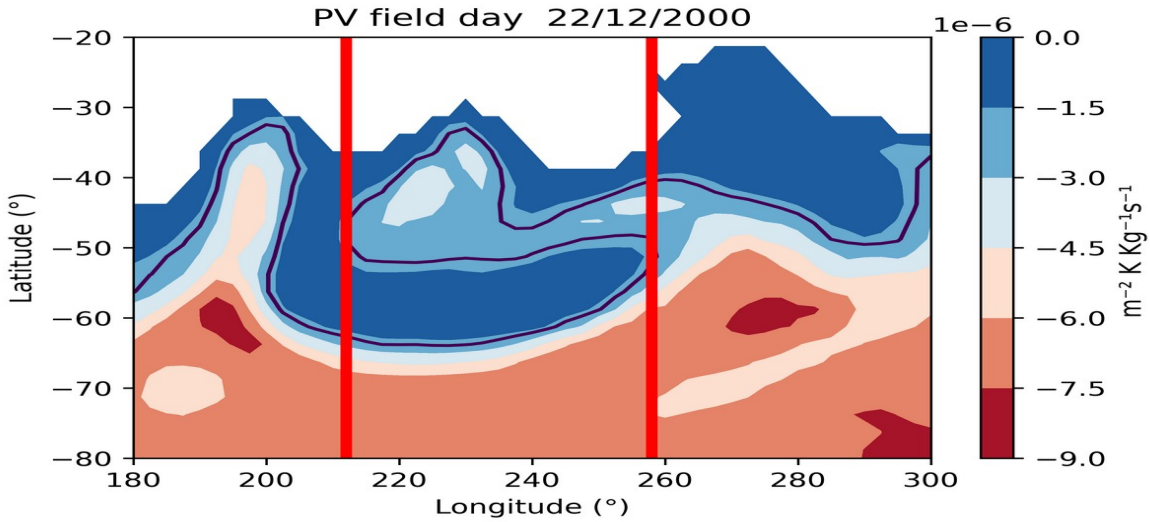

Figure 1. Potential vorticity fields following the 330ºK isentropic isosurface during an anticyclonic RWB event detected on 22/12/2000. Red lines indicate the longitudinal section where the algorithm found the RWB event and the black line signals the location of the -2PVU line.

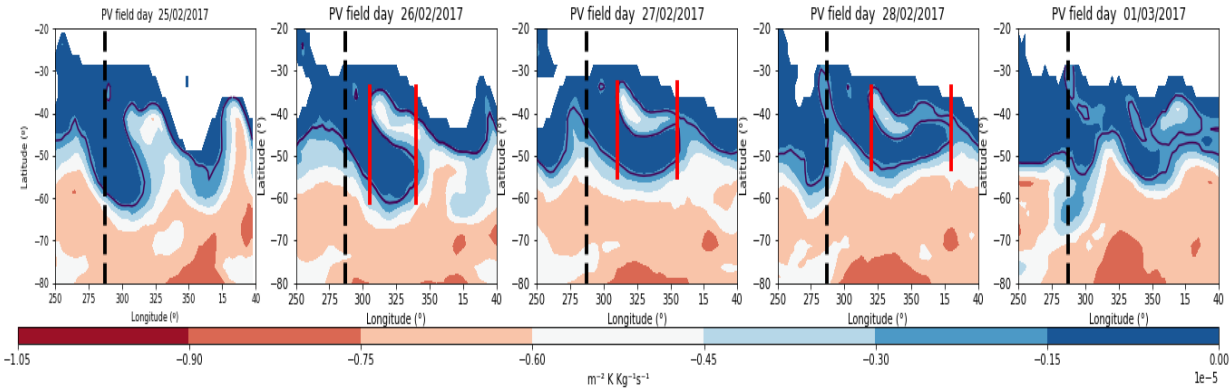

Figure 2. Potential vorticity fields following the 330ºK isosurface between 25/02/2017-01/03/2017. The dashed black line shows the longitudinal section where a LLRWPs stopped its propagation at 25/02/2017, red lines indicate the area of RWB detected by the wave breaking algorithm and the black line signals the location of the -2PVU line.

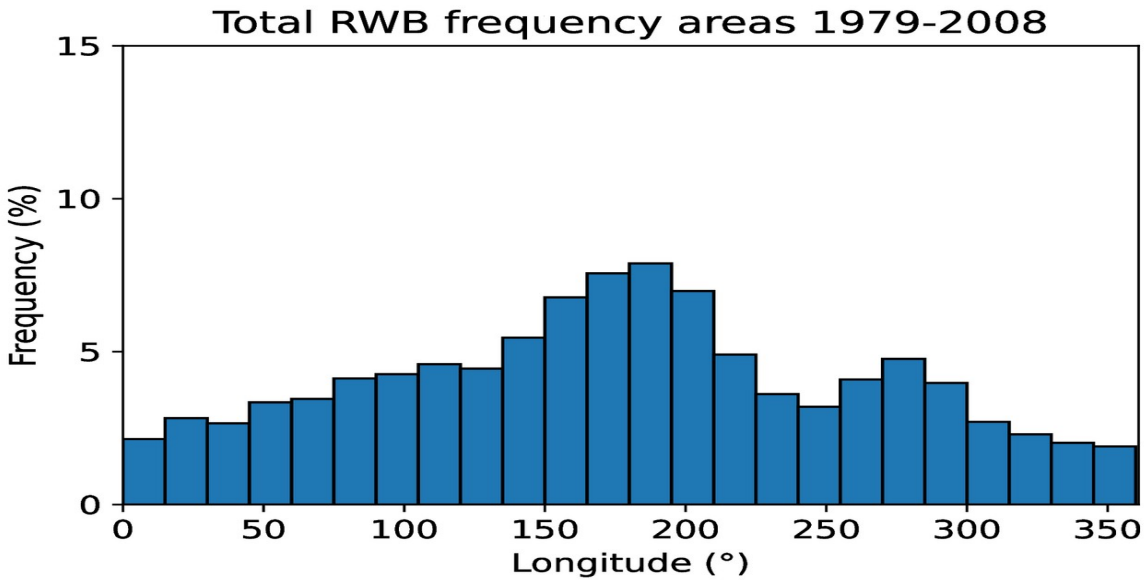

Figure 3. Frequency of RWB events found during summertime in the Southern Hemisphere between 1979-2008.

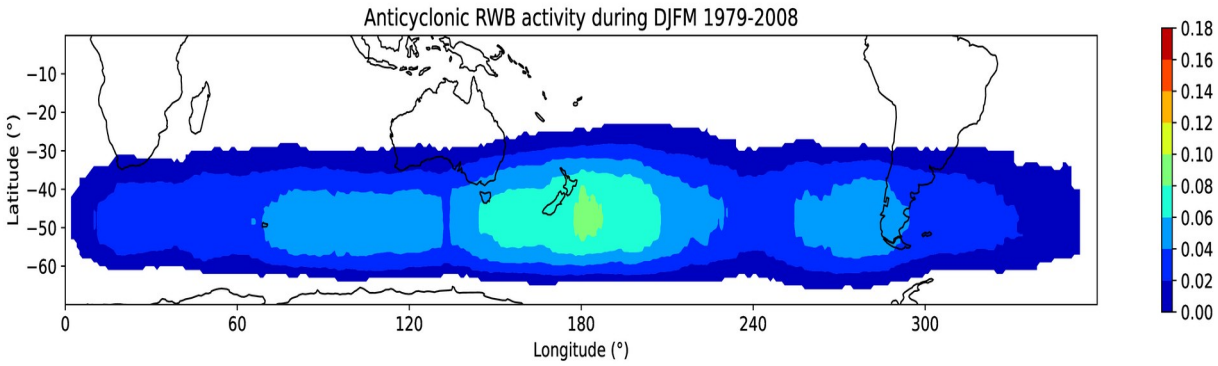

Figure 4. Anticyclonic RWB frequency found between 1979-2008. Colored areas show where RWB episodes where detected.

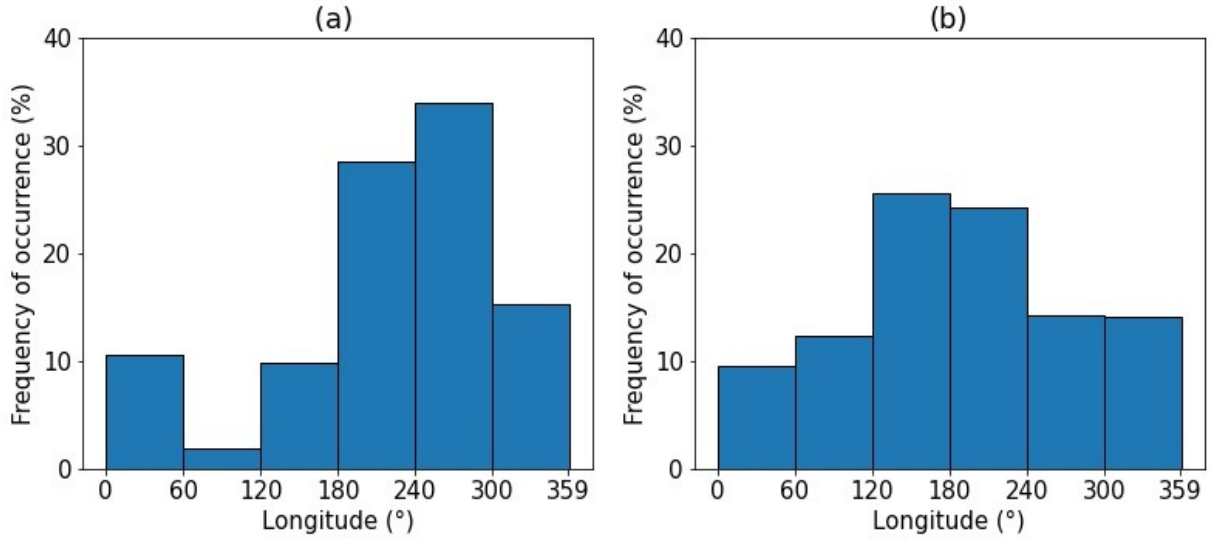

Figure 5. Relative frequency of occurrence of large-scale RWB associated to (a) LLRWPs and (b) SLRWPs.

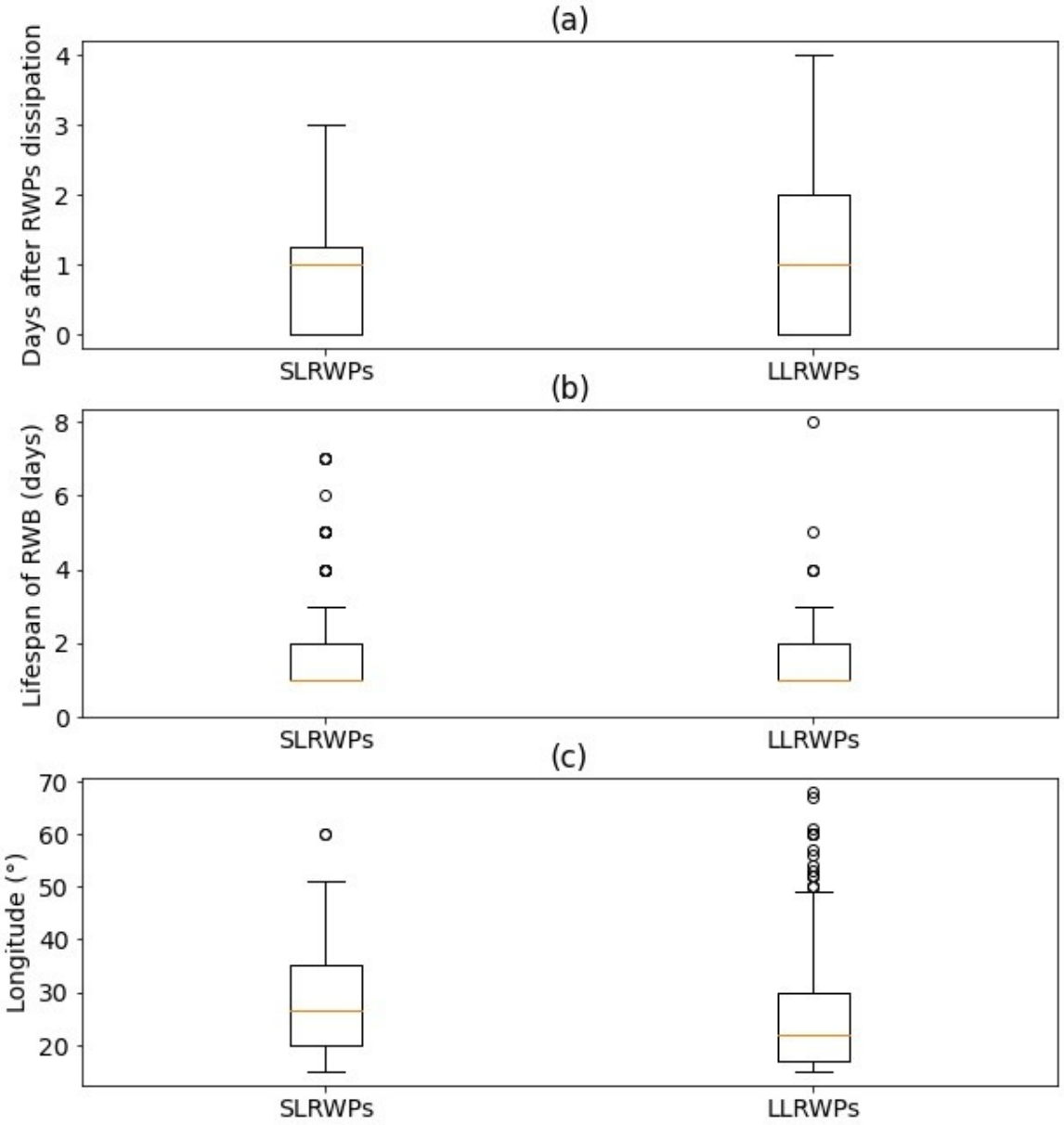

Figure 6. Boxplot distribution of several characteristics of RWB associated with LLRWPs and SLRWPs. Yellow lines in the boxplots signal the location of the median of the distribution. Upper figure (a) shows the day when a large-scale RWB event appears after the end of the RWPs propagation, middle figure (b) displays the mean lifespan of the RWB events, whereas the last figure shows the longitudinal extension of the RWB.

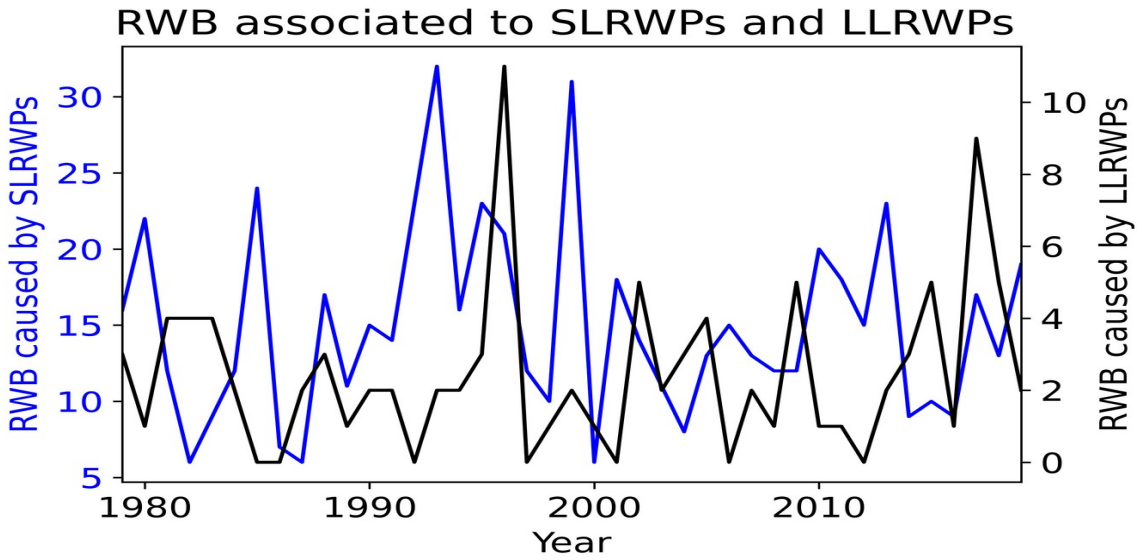

Figure 7. Interannual variability of RWB events associated to LLRWPs (black) and SLRWPs (black lines).

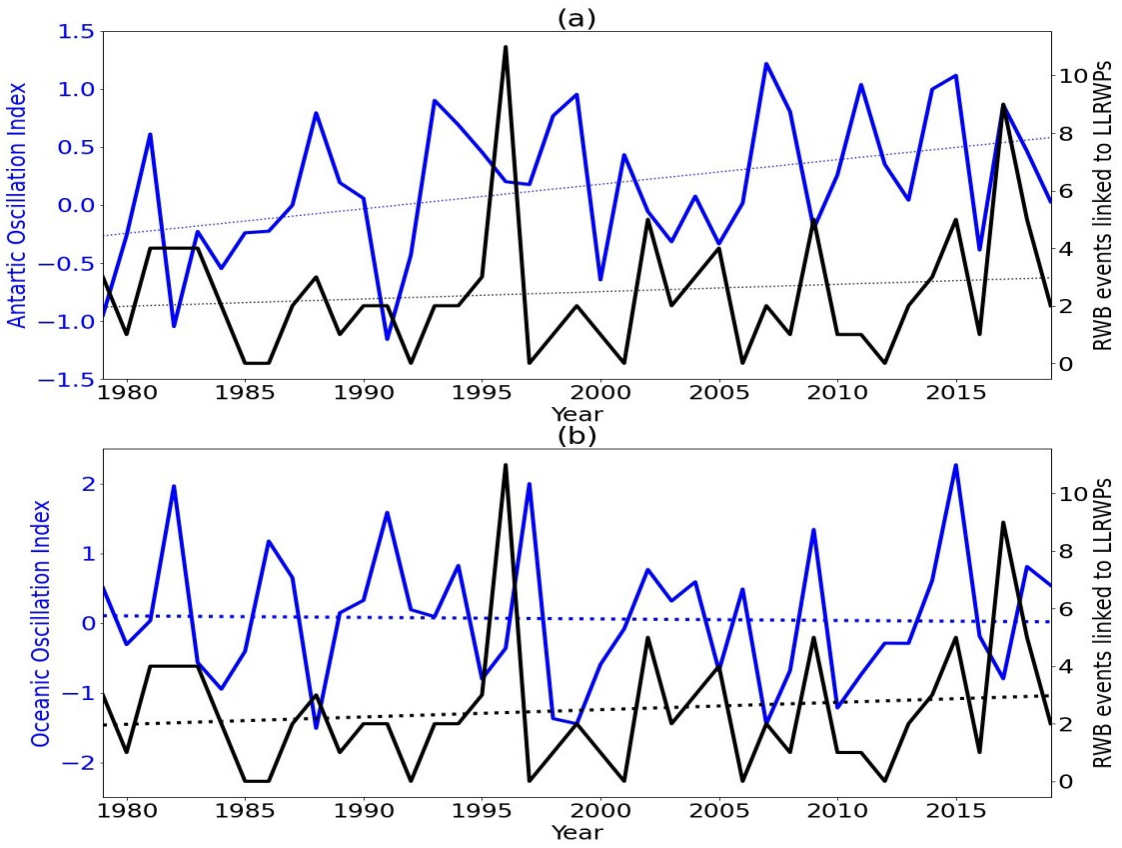

Figure 8. Timeseries of annual RWB events associated to LLRWPs (black lines), against the temporal evolution of Oceanic Niño Index (a) and Antarctic Oscillation Index (b) during the period of study (blue lines). Dotted lines show the trend for each timeseries.

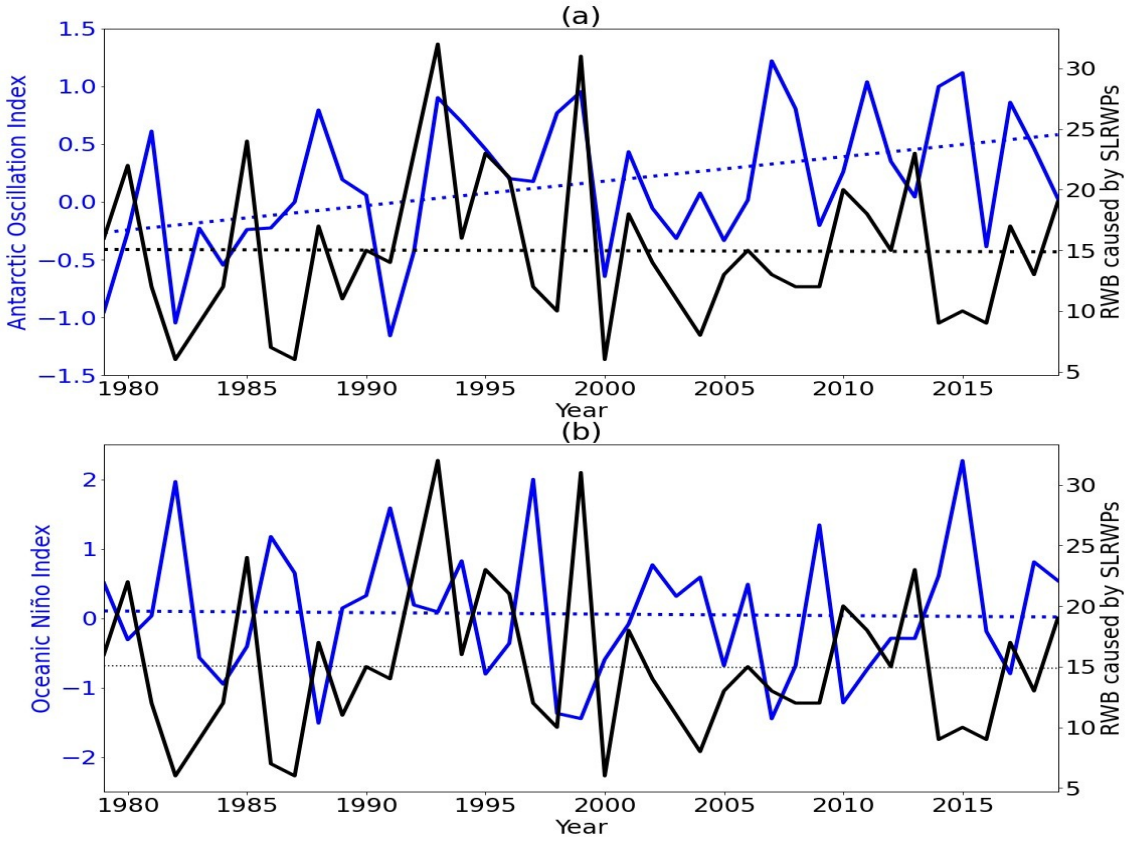

Figure 9. Timeseries of annual RWB events associated to SLRWPs (black lines), against the temporal evolution of Oceanic Niño Index (a) and Antarctic Oscillation Index (b) during the period of study (blue lines). Dotted lines show the trend for each timeseries.